Abnormal Tibia Translation leads Directly the Surface Cartilage Degeneration with Molecular Biological Response using a Novel Non-Invasive ACL ruptured Mice Model

Kei Takahata M.Sc.[1,2], Kohei Arakawa M.Sc.[1], Saaya Enomoto[3], Yuna Usami[3], Koyo Nogi[3], Kaichi Ozone Ph.D.[4], Haruna Takahashi M.Sc.[1], Moe Yoneno M.Sc.[1], Takanori Kokubun Ph.D.[1,3.]

1: Department of Health and Social Services, Health and Social Services, Graduate School of Saitama Prefectural University, Saitama, Japan
2: Japan Society for the Promotion of Science, Tokyo, Japan
3: Department of Physical Therapy, Health and Social Services, Saitama Prefectural University, Saitama, Japan
4: University of Tsukuba Hospital, Ibaraki, Japan

Corresponding author: Takanori Kokubun, PhD
Department of Physical Therapy, Health and Social Services, Saitama Prefectural University Saitama, Japan
E-mail: kokubun-takanori@spu.ac.jp

Authors' email addresses:
Kei T; 2491006o@spu.ac.jp
Kohei A; 2391001y@spu.ac.jp
Saaya E; 2481302r@spu.ac.jp
Yuna U; 2381301n@spu.ac.jp
Koyo N; 2481312s@spu.ac.jp
Kaichi O; 2191002a@spu.ac.jp
Haruna T; 2491005w@spu.ac.jp
Moe Y; 2491010y@spu.ac.jp
Takanori K; kokubun-takanori@spu.ac.jp

Abstract

Objective:

Mechanical stress is one of the most exacerbating factors on knee osteoarthritis (OA). We recently reported the effect of shear stress on OA progression in vivo using controlled abnormal tibial translation (CATT), which suppressed shear stress in vivo due to ACL transection (ACL-T). However, surgical ACL-T mice models were used, thus effect of shear stress cannot be clarified exactly. So, we aimed to establish a novel Non-Invasive ACL-T without intra-articular injuries and reveal the onset mechanism of knee OA induced by shear stress.

Design:

First, twelve-week-old C57BL/6 male mice were used to make a novel Non-Invasive ACL-T model. After creating the model, injuries of intra-articular tissues were observed histologically, macroscopically, and morphologically. Next, twelve-week-old C57BL/6 male mice were categorized into ACL-T, CATT, and Sham groups. After 2,4 and 8 weeks, we performed the anterior drawer test, safranin-O/fast green staining, and immunohistochemical staining for MMP-3 and TNF-α.

Results:

In a novel Non-Invasive ACL-T model, no injuries, including cartilage, meniscus, and bone were not observed except ACL rupture. Regarding OA progression, the anterior tibial translation in the ACL-T group was significantly higher than that of the other groups at all weeks, and cartilage degeneration in the ACL-T group increased significantly compared with the other groups at 8 weeks. Although synovitis score in the ACL-T and CATT groups was significantly higher than the Sham group at 2 and 8 weeks, there were no differences between the ACL-T and CATT groups. In addition, the MMP-3 positive cell rate in the cartilage of the ACL-T group was higher than the other groups at 4 and 8 weeks. However, that in the synovium of the ACL-T group was higher than the other groups at 8 weeks. TNF-α positive cell rates in both cartilage and synovium were not changed between the ACL-T and CATT groups.

Conclusion:

We have successfully established a new Non-Invasive ACL-T model without intra-articular tissue damage, which induces knee OA due to shear stress. In the OA progression caused by shear stress, chondrocytes first showed a molecular biological

response, leading to a local increase in MMP-3. On the other hand, synovitis is not directly induced by mechanical stress but is indirectly caused by intra-articular degeneration associated with knee OA progression.

Introduction

Knee Osteoarthritis (OA) is a multifactorial disease caused by various factors; aging, obesity, and mechanical stress. These factors are attracting attention as a significant pathogenic factor recently. When physiological mechanical stress is applied, chondrocytes promote the extracellular matrix synthesis and suppress inflammatory factors, and homeostasis is maintained[1)]. On the other hand, when abnormal mechanical stress accumulates, a disintegrin and metalloproteinase with thrombospondinemotifis (ADAMTS-4,5) and Matrix Metalloproteinase (MMP-1,3,13) cause degeneration of articular cartilage by proteoglycan and type II collagen degradation[2-4)].

Since the knee joint is a synovial joint sealed by the joint capsule, intra-articular tissues such as articular cartilage and synovial membrane have biological interactions with synovial fluid[5-9)]. Synovitis is one of the intra-articular pathologies involved in OA, which contributes to cartilage degradation by releasing proinflammatory and catabolic products into synovial fluid[10)]. Some previous studies reported that synovitis occurs relatively early and causes cartilage degeneration[11,12)]. However, the relationship between these two pathologies has not been elucidated in detail under mechanical stress.

Many animal OA models have been developed to elucidate the mechanism of knee OA induced by mechanical stress, and a representative one is ACL-Transection (ACL-T) model. We recently reported a joint-controlled model, controlled abnormal tibial translation (CATT)[13)], which suppresses shear stress in vivo due to ACL-T. In addition, we established another joint-controlled model, called the controlled abnormal tibial rotation (CATR) model that suppress abnormal joint rotation due to destabilization of the medial meniscus (DMM)[14)]. Using these models, Arakawa et al. revealed that the difference in mechanical stress types, such as compression and shear stress, had a different effect on joint degeneration[15)]. In particular, it was suggested that shear stress in the ACL-T model causes articular cartilage degeneration by inducing chondrocyte hypertrophy compared to the CATT model.

However, in the previous study, we used surgical intervention to create the ACL-T model. Thus, synovium invasion might disrupt the natural intra-articular environment of the knee joint. Therefore, it comes with unintended adaptive and healing processes due to the invasion itself. To avoid these problems in surgical OA models, many researchers

tried to establish the Non-invasive ACL-T OA models[16-18]. Christiansen et al. reported that mice's knee and ankle joints are fixed with a device, and the tibia is compressed toward the knee joint surface to induce ACL rupture. However, conventional Non-invasive ACL-T OA models focused on the effect of cartilage compression stress in the OA progression. Since these models were created using compression stress for the knee joint surface and induced anterior tibial dislocation. Besides not only inducing the shear stress due to ACL-T, primary injury of cartilage, meniscus, and subchondral bone could occur when it was made in conventional Non-invasive ACL-T models.

Therefore, this study aimed to establish a novel, Non-Invasive ACL-T knee OA model that avoids injury to intra-articular tissues except the ACL rupture. We manually applied the anterior tibial translation stress to rupture the ACL without any contact between the tibia plateau and femur condyle. Comparing this model with the CATT model, we tried to reveal that the onset mechanism of knee OA induced by shear stress with ACL rupture can be clarified more precisely, especially in synovitis.

Material and Methods

Animals and experimental design

The Animal Research Committee of Saitama Prefectural University approved this study (approval number: 2020-6). The animals were handled according to the relevant legislation and institutional guidelines for humane animal treatment. In this study, 18 C57BL/6 male mice were first used to evaluate the methods to make a novel Non-Invasive ACL-T model and whether there were any injuries to intra-articular tissues. The contralateral knee joint was used as the INTACT group (Fig 1[A]). Then, 54 mice were randomly classified into three groups: ACL-T group (n=18; shear stress increases by ACL rupture), CATT group (n=18; shear stress with ACL rupture is suppressed by external support), and Sham group (n=18). Six mice in each group were sacrificed at 2, 4, and 8 weeks, and the target tissues were collected for each analysis (Fig 1[B]). All mice were housed in plastic cages, and the room had a 12-hour light/dark cycle. Mice were allowed unrestricted movement within the cage and had free access to food and water.

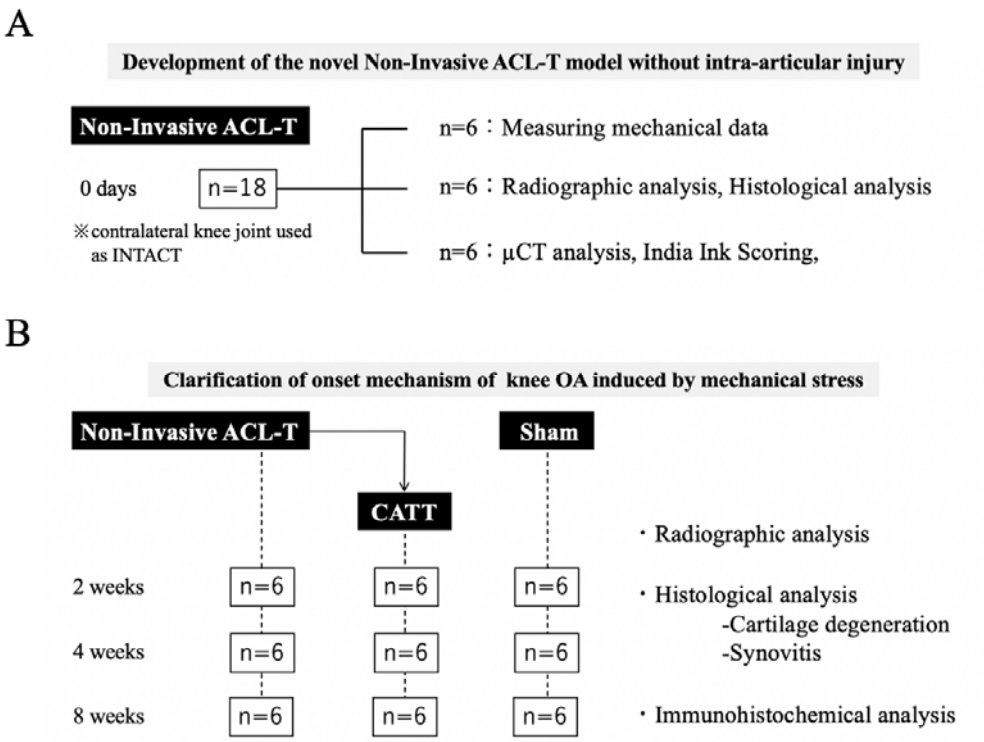

Figure 1. Experimental design. (A) Development of the novel Non-Invasive ACL-T model without intra-articular injury. We created the Non-Invasive ACL-T model and performed a biomechanical investigation and histological, morphological, and macroscopical analyses to evaluate intra-articular injuries except ACL rupture. (B) Clarification of onset mechanism of knee OA induced by shear stress. Non-Invasive ACL-T group, CATT group, and Sham group were sacrificed at 2, 4, and 8 weeks and assessed the degree of OA progression through validity investigation and histological analyses.

Development of the novel Non-Invasive ACL-T model without intra-articular injury

Creating model procedure

All procedures were performed on the left knee joint under a combination anesthetic (medetomidine, 0.375 mg/kg; midazolam, 2.0 mg/kg; and butorphanol, 2.5 mg/kg). The knee joint was fixed at 90 degrees using surgical tape on a stand. The femoral condyle was pushed manually in the long axis direction, causing ACL rupture due to relative anterior dislocation of the tibia. To evaluate the intra-articular injuries without ACL injury, we collected the knee joints 0 days after creating the model and performed the following analyses (Fig. 2[A]).

Calculating the force of ACL rupture

To assess the force of ACL rupture in a Non-Invasive ACL-T model, the ACL-T model was created using MINI LOAD CELL (MDB-25; Transducer Techniques, CA, USA), and the mechanical data was measured. The data was transmitted to the PC via the load cell amplifier and was processed using Arduino software, version 1.8.16, and Jupyter Lab software, 1.1.4 to calculate the force and speed of ACL rupture (Fig. 2[B]).

Radiographic analysis

We performed the anterior drawer test and measured anterior tibial displacement to evaluate shear stress on the joint surface through the manual ACL rupture. Based on the previous study[15)], the tibia's anterior displacement was quantified using Image J (ImageJ; National Institutes of Health, Bethesda, MD, USA).

Histological analysis

The knee joints were fixed with 4% paraformaldehyde for 1 day, decalcification in 10% ethylenediaminetetraacetic acid for 2 weeks, dehydrated, and embedded in paraffin. The samples were cut in the sagittal plane (7 mm thickness) using a microtome (ROM-360; Yamato Kohki Industrial Co., Ltd., Saitama, Japan). Hematoxylin and Eosin (H&E) staining was performed to observe the ACL rupture, and Safranin-O/fast green staining was performed to evaluate the articular cartilage and meniscus injuries.

Micro-computed tomography (µCT) analysis

To evaluate morphological changes in whole knee joints and subchondral bone, we collected knee joints and stored them at -80℃ until analyzed. The knee joints were scanned using a µCT system (Skyscan 1272, BRUKER, MA, USA) with the following parameters: pixel size, 6 mm; voltage, 60 kV; current, 165 mA. Subsequently, the reconstructed image was acquired using the NRecon software (BRUKER, MA, USA). For morphological analysis of subchondral bone, the regions of interest were defined as MFC, LFC, MTC, and LTC to the growth plate. Then, we calculated the bone volume/tissue volume fraction (BV/TV, %), trabecular thickness (Tb. Th, mm), trabecular number (Tb. N, 1/mm), and trabecular separation (Tb. Sp, mm) using CTAn software (BRUKER, MA, USA). In addition, the reconstructed image showed bone loss and detachment fracture of ACL macroscopically.

Macroscopic Observation analysis

After μCT analysis, the tibial plateau was carefully separated from the femoral condyle, and these tissues were stained with India ink[19] to visualize the damaged region on the joint surface. Macroscopic pictures of the femoral and tibial condyles were taken using a stereomicroscope SZX10 (Olympus Co., Ltd., Tokyo, Japan) on a platform. Based on a previous study, the cartilage injury on the medial femoral condyle (MFC), lateral femoral condyle (LFC), medial tibial condyle (MTC), and lateral tibial condyle (LTC) were evaluated using a macroscopic score on a scale of 0-5 points.

Clarification of the onset mechanism of knee OA induced by shear stress

Creating model procedure

The non-Invasive ACL-T model was created as described above, and the CATT model was created following the previous study[15]. After making the Non-Invasive ACL-T model, we create extra-articular bone tunnels in the distal femur and proximal tibia using a 26-gauge needle. Then 4-0 nylon sutures were threaded through them and suppressed the forward displacement of the tibia from outside the joint capsule. To standardize the conditions for model fabrication, bone tunnels were also created in the Sham and ACL-T groups, and nylon threads were loosely tied to prevent suppressing joints. After creating each model, we collected the knee joints at 2, 4, and 8 weeks and performed the following analyses.

Radiographic analysis

To evaluate reproduce of shear stress in vivo, the knee joints anterior drawer test was performed as described above, and the amount of anterior displacement of the tibia was quantified.

Histological analysis

We performed Safranin-O/fast green staining to evaluate articular cartilage degeneration and synovitis with OA progression histologically. The Osteoarthritis Research Society International (OARSI) histopathological grading system[20] and synovitis score[21] were used to assess by two independent observers blinded to all other sample information. The contact area not covered by the meniscus on the MTC was used for the OARSI score. The medial synovium located inside the infrapatellar pad was used for the synovitis score. Then, the mean of the observer's scores was used as the representative value.

Immunohistochemical analysis

To assess the expression of Matrix metalloproteinase-3 (MMP-3) and Tumor Necrosis Factor-a (TNF-a) immunohistochemical staining using the avidin-biotinylated enzyme complex method and the VECTASTAIN Elite ABC Rabbit IgG Kit (Vector Laboratories, Burlingame, CA, USA) was performed. We used anti-MMP-3 (1:100, ab52915, Abcam) and TNF-a (1:200, bs-1110R, Bioss) as the primary antibody and anti-rabbit IgG antibody as the secondary antibody. The sections were then stained using the Dako Liquid DAB þ Substrate Chromogen System (Dako, Glostrup, Denmark). Cell nuclei were stained with hematoxylin at a 25% concentration.

We calculated the ratio between MMP-3 and TNF-a positive cells and the number of chondrocytes in an articular cartilage area and synovial cells in a synovial area of 10,000 mm^2 (100 μm × 100 μm).

Statically analysis

Statistical analysis of the measured data was performed using R software, version 3.6.1. The Shapiro-Wilk test verified the normality of all analyzed data. We conducted a t-test for the anterior drawer test immediately after creating a Non-Invasive model. India Ink Scoring, BV/TV, Tb.Th, Tb.N, and Tb.Sp. The Wilcoxon rank-sum test was analyzed in the subchondral bone. A one-way analysis of variance (ANOVA) was performed for the anterior drawer test at 2, 4, and 8 weeks. The comparison of MMP-3 and TNF-α positive cells rate on articular cartilage and synovium and the Tukey-Kramer test was used for multiple comparisons.

Meanwhile, the Kruskal-Wallis test was performed comparing OARSI scores and synovitis scores, and the Steel-Dwass method was used for subsequent multiple comparisons. Parametric data were expressed as means with 95% confidence intervals (CI), whereas non-parametric data were expressed as medians with interquartile ranges. The statistical significance was set at $P < 0.05$.

Result

Development of the novel Non-Invasive ACL-T model without intra-articular injury

Measurement of ACL rupture force

To reveal the mechanical data, the force of ACL rupture and time data were measured using a load cell during the creation of a novel, Non-Invasive ACL-T model.

The maximum force was 7.11±0.45 N, and the time taken for rupture was 1.90±0.79 sec; the rupture speed derived from these results was 4.09±1.21 N/s (Fig. 2[B]).

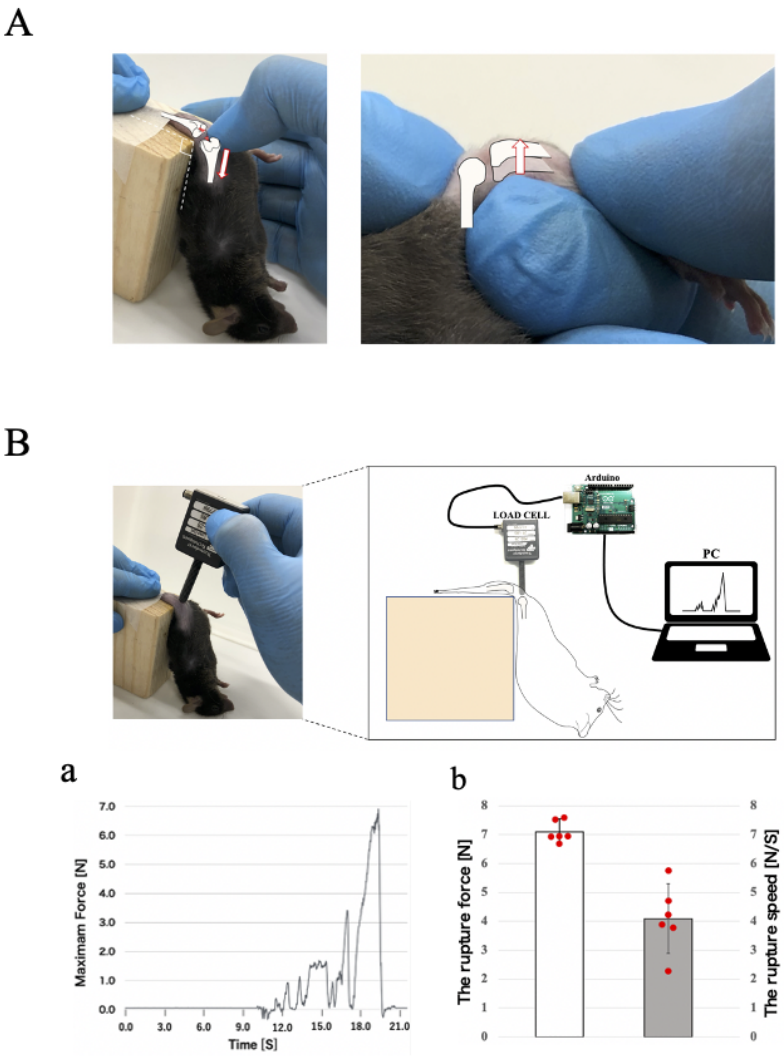

Figure 2. (A) Novel Non-Invasive ACL-T model. We fixed the knee joints at 90 degrees, pushed the femoral condyle manually on the long axis, and then confirmed ACL rupture with anterior tibial displacement. (B) Mechanical data of ACL rupture. Using MINI LOAD CELL and Arduino, the longitudinal mechanical data during ACL rupture was measured (a). Then, the ACL rupture force and rupture speed were calculated. Data are presented as the mean with a 95% CI.

Anterior tibial displacement was confirmed in the Non-Invasive ACL-T model.

The soft X-ray images of knee joints during the anterior drawer test after creating the Non-Invasive ACL-T model are shown in Fig 3(A). Compared to the INTACT group, an obvious abnormality in the tibial position was observed, and the anterior tibial displacement significantly increased in the ACL-T group ($p<0.001$, 95%CI [0.824 - 1.126]).

No soft tissue injuries except ACL rupture were detected histologically.

Histological images of the knee joint by H&E and Safranin O/fast-green staining are shown in Fig 3(B). ACL with uniform collagen orientation and cell arrangement was observed in the INTACT group, whereas ACL disrupted continuity and abnormal anterior tibial displacement were observed in the ACL-T group. Regarding the joint's surface, no damage was found in the soft tissues such as the surface layer of articular cartilage and meniscus in a medial and lateral compartment in both INTACT and ACL-T groups.

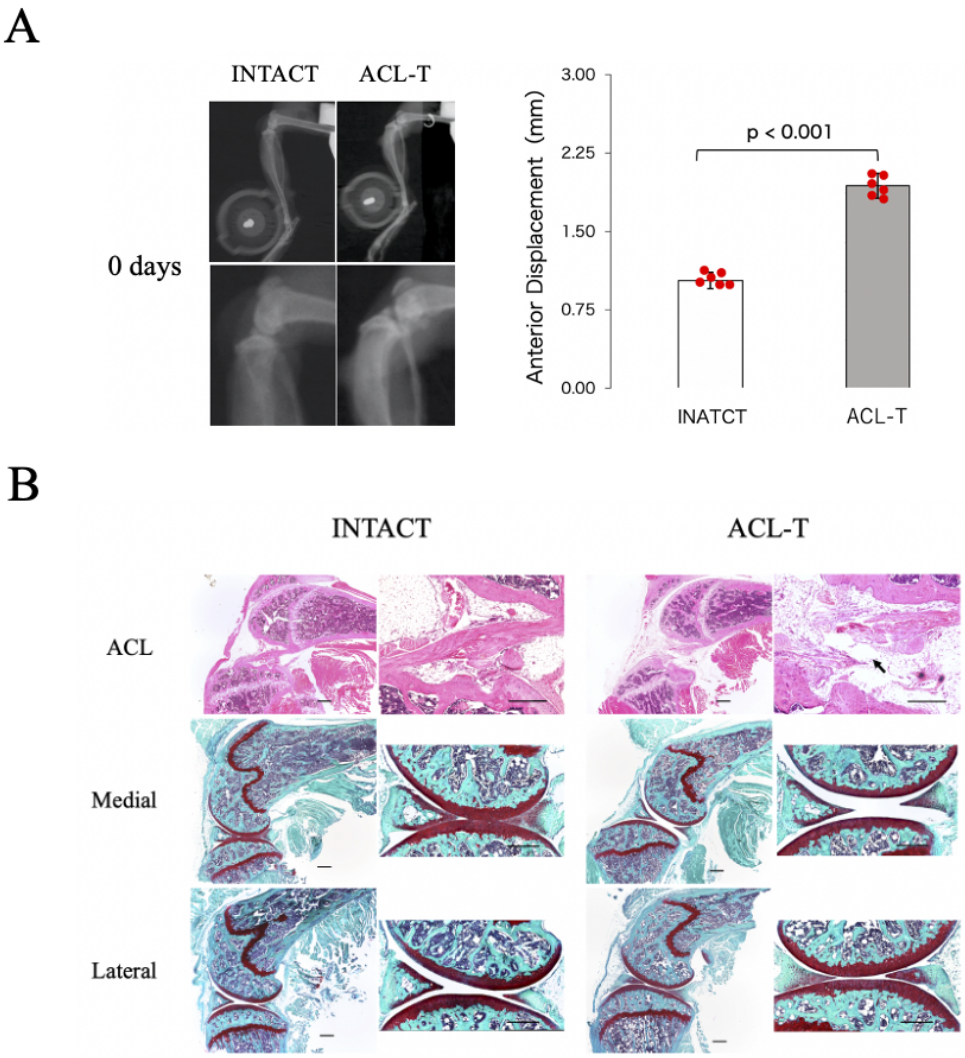

Figure 3. (A) Evaluation of ACL rupture using soft x-ray device. The anterior tibial displacement was significantly increased in the Non-Invasive ACL-T group compared to the INTACT group. Data are presented as the mean with a 95% CI. (B) Histological analysis for intra-articular tissues with H&E staining and Safranin-O/fast green staining. In the INTACT group, no injury was detected in ACL, cartilage, and meniscus. In the Non-Invasive ACL-T group, only ruptured ACL was confirmed, but no articular cartilage or meniscus injuries were observed. Black scale bar, 300 µm. Black arrows show disrupted continuity in ACL.

No morphological changes in whole knee joints and subchondral bone have been observed.

The 3D reconstruction images of the knee joint by μCT analysis and morphological analysis of subchondral bone are shown in Fig 4(A). In the ACL-T group, no obvious bone loss and no avulsion fracture of the ACL attachment was observed. In addition, there were no significant differences in BV/TV, Tb.Th, Tb.N, and Tb.Sp in each compartment of both INTACT and ACL-T groups.

No injury to joint surfaces has been detected with India Ink.

The macroscopic images of the articular surface and results of India Ink Scoring are shown in Fig 4(B). Partial staining was observed in each compartment of both INTACT and ACL-T groups; however, no significant difference was observed between the groups in each compartment.

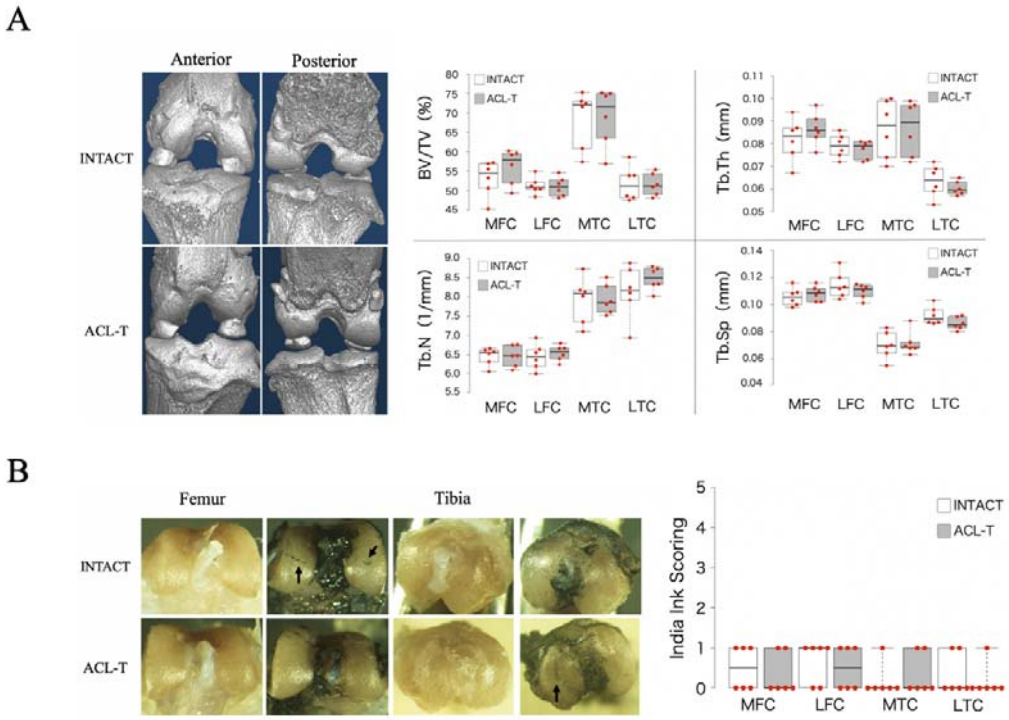

Figure 4. (A) The 3D images of the whole knee joint and morphological analysis of subchondral bone by μCT. No bone loss and microfracture were observed in the Non-Invasive ACL-T group. Besides, there were no differences in BV/TV, Tb.Th, Tb.N, and Tb.Sp in MFC, LFC, MTC, and LTC between the INTACT and the ACL-T groups. Data are presented as the median with an interquartile range. (B) The macroscopic images of joint surface with India Ink staining. There were no differences between the INTACT and the ACL-T groups in MFC, LFC, MTC, and LTC. Data are presented as the median with an interquartile range. Black arrows show punctate depressions.

Clarification of the onset mechanism of Knee OA induced by shear stress

Anterior Drawer Test

To evaluate the validity of each model, we performed an anterior drawer test and quantified the amount of anterior tibial dislocation (Fig 5). At 2 weeks, the anterior displacement in the ACL-T group was significantly increased compared with the Sham and the CATT groups ([ACL-T vs. Sham]; p<0.001, 95%CI [-1.482 to -0.897], [ACL-T vs. CATT]; p<0.001, 95%CI [-1.211 to -0.625]). At 4 weeks, the anterior displacement in the ACL-T group was significantly increased compared with the Sham and CATT groups ([ACL-T vs. Sham]; p<0.001, 95%CI [-1.508 to -0.871], [ACL-T vs. CATT]; p<0.001, 95%CI [-1.252 to -0.614]). At 8 weeks, the anterior displacement in the ACL-T group increased significantly compared with the Sham and CATT groups ([ACL-T vs. Sham]; p<0.001, 95%CI [-1.509 to -0.966], [ACL-T vs. CATT]; p<0.001, 95%CI [-0.841 to -0.298]) and the CATT group also increased significantly compared with the Sham group (p<0.001, 95%CI [-0.939 to -0.396]).

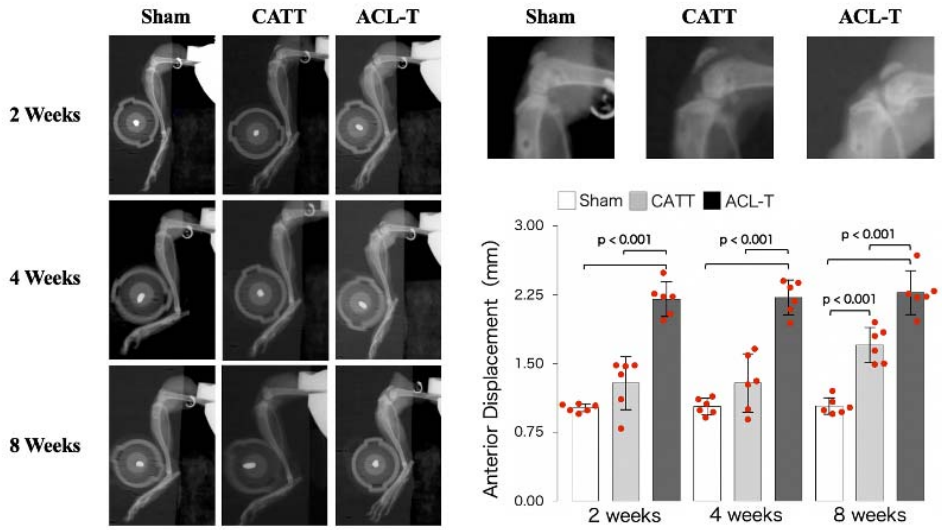

Figure 5. Evaluation of shear stress in vivo using soft x-ray analysis. At 2, 4, and 8 weeks, the amount of anterior tibial displacement was significantly increased in the ACL-T group compared with the Sham and the CATT groups. Data are presented as the mean with a 95% CI.

Histological analysis of cartilage degeneration

Safranin-O/fast green staining image and the result of the OARSI score are shown in Fig 6(A). Staining intensity of safranin O in the surface layer of articular cartilage was decreased in all groups at 2 weeks. Irregularities and fibrillation of the articular cartilage surface were observed in the CATT and ACL-T groups but not in the Sham group at 4 weeks. However, there was no significant difference in OARSI scores at 2 and 4 weeks.

At 8 weeks, partial clefts and erosion in the surface layer of articular cartilage were observed in the CATT group, vertical cracks and massive erosion in the calcified cartilage layer were observed in the ACL-T group, and the OARSI score in the ACL-T group increased significantly compared with the Sham and CATT groups ([ACL-T vs. Sham]; p=0.004, [ACL-T vs. CATT]; p=0.006) and the CATT group increased significantly compared with the Sham group (p=0.003).

Histological analysis of synovitis

Safranin-O/fast green staining image and the result of synovitis score are shown in Fig 6(B). At 2 weeks, moderate enlargement of the synovial lining cell layer and increased cellularity of the synovial stroma were observed in the CATT and ACL-T groups. The synovitis score of the CATT and ACL-T groups increased significantly compared with the Sham group ([CATT vs. Sham]; p=0.033, [ACL-T vs. Sham]; p=0.026). However, there was no significant difference between CATT and ACLT groups.

At 4 weeks, although mild enlargement and increased cellularity were observed in the CATT and ACL-T groups, synovitis score was no significant difference. At 8 weeks, the CATT and ACL-T groups showed severe enlargement of the synovial lining cell layer, increased interstitial cellularity, and inflammatory infiltrates. The synovitis score of the CATT and ACL-T groups increased significantly compared with the Sham group ([CATT vs. Sham]; p=0.008, [ACL-T vs. Sham]; p=0.008). However, there was no significant difference between CATT and ACLT groups.

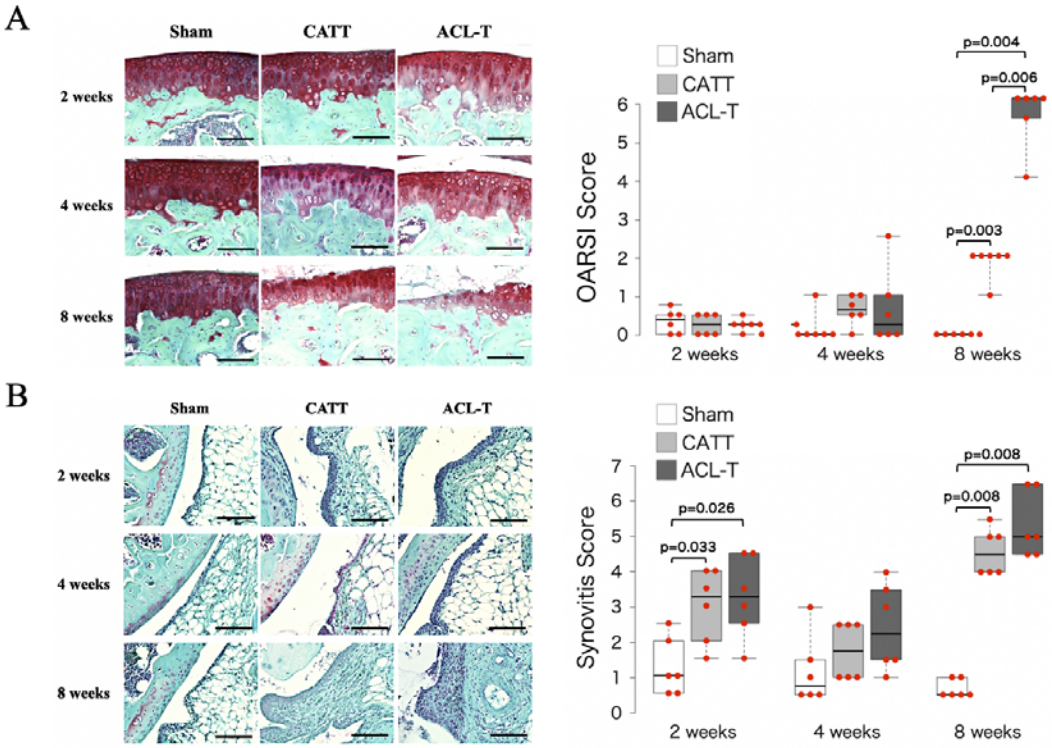

Figure 6. (A) Histological analysis for cartilage degeneration with Safranin-O/fast green staining and OARSI score. At 8 weeks in the CATT group, moderate cartilage degeneration was observed, and the OARSI score was significantly increased compared to the Sham group. At 8 weeks in the ACL-T group, severe cartilage degeneration was observed, and the OARSI score was significantly increased compared with the Sham and the CATT groups. Data are presented as the median with an interquartile range. Black scale bar, 100 µm. (B) Histological analysis for synovitis with Safranin-O/fast green staining and synovitis score. At 2 weeks in the CATT and ACL-T groups, moderate enlargement of the synovial layer and increased synovial cellularity were observed, and synovitis score increased significantly compared to the Sham group. At 8 weeks in the CATT and ACL-T groups, severe enlargement of the synovial layer increased synovial cellularity, and inflammatory infiltrates were observed. Synovitis score increased significantly compared to the Sham group. Data are presented as the median with an interquartile range: Black scale bar, 100 µm.

Immunohistochemical analysis of articular cartilage and synovium

The results of immunohistochemical staining in articular cartilage and the analysis of positive cell rate are shown in Fig 7. At 2 weeks, there were no significant differences in the positive cell rate of MMP-3 between all groups. At 4 weeks, the MMP-3 positive cell rate in the ACL-T group was significantly increased compared with the Sham and

the CATT groups ([ACL-T vs. Sham]; p=0.001, 95%CI [-37.44 to -9.485], [ACL-T vs. CATT]; p=0.043, 95%CI [-28.32 to -0.364]). At 8 weeks, the positive cell rate of MMP-3 in the ACL-T group was significantly increased compared with the Sham and the CATT groups ([ACL-T vs. Sham]; p<0.001, 95%CI [-36.363 to -13.986], [ACL-T vs. CATT]; p=0.031, 95%CI [-23.398 to -1.021]), and that in the CATT group was significantly increased compared with the Sham group([CATT vs. Sham]; p=0.022, 95%CI [-24.153 to -1.776]) [Fig 7 (A)]. Regarding the positive cell rate of TNF-a, there were no significant differences between all groups at 2, 4, and 8 weeks [Fig 7 (B)].

Next, the results of immunohistochemical staining in synovium and the analysis of positive cell rate are shown in Fig 8. At 2 weeks, there were no significant differences in the positive cell rate of MMP-3 between all groups. At 4 weeks, the MMP-3 positive cell rate in the ACL-T group was significantly increased compared with the Sham group (p=0.014, 95%CI [-27.612 to -3.01]). At 8 weeks, the positive cell rate of MMP-3 in the ACL-T group was significantly increased compared with the Sham and the CATT groups ([ACL-T vs. Sham]; p<0.001, 95%CI [-34.197 to -15.782], [ACL-T vs. CATT]; p=0.042, 95%CI [-18.697 to -0.282]), and that in the CATT group was significantly increased compared with the Sham group([CATT vs. Sham]; p=0.001, 95%CI [-24.707 to -6.292]) [Fig 8 (A)]. There was no significant difference in the positive cell rate of TNF-a at 2 weeks, but the ACLT group increased more than the other groups, and the CATT group increased more than the Sham group. At 4 weeks, there was no significant difference in the positive cell rate of TNF-a between all groups. At 8 weeks, the positive cell rate of TNF-a in the CATT and ACL-T groups was significantly increased compared with the Sham group ([CATT vs. Sham]; p=0.032, 95%CI [-31.833 to -1.354], [ACL-T vs. Sham]; p=0.011, 95%CI [-34.826 to -4.347]) [Fig 8 (B)]. （1152 words）

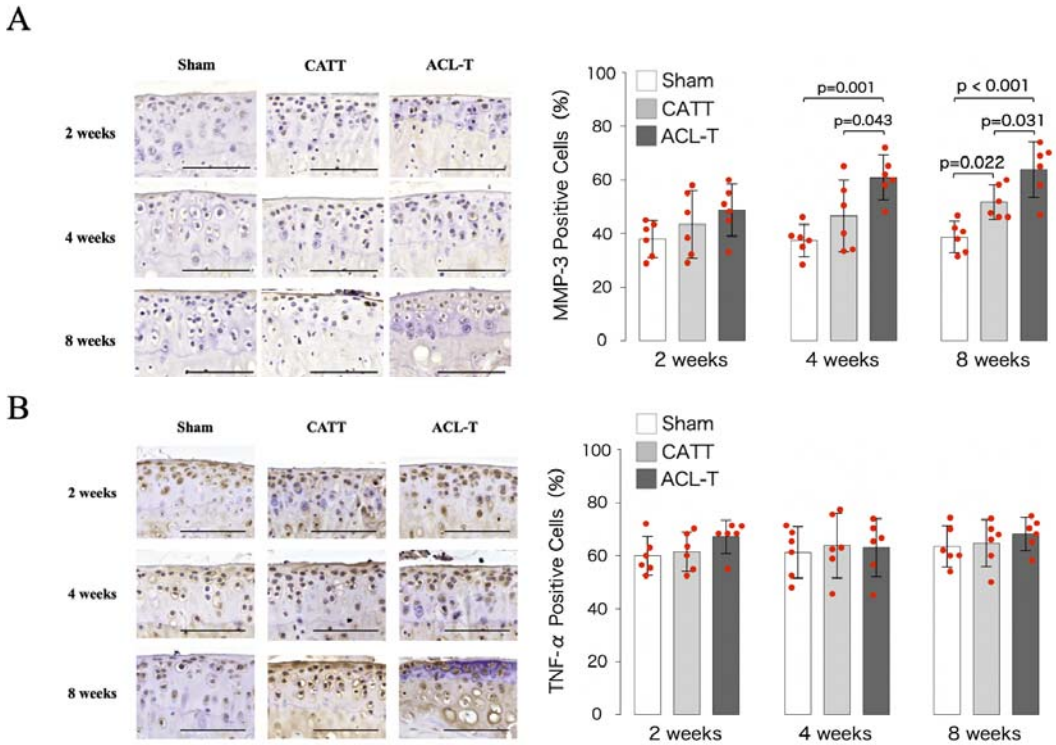

Figure 7. (A) Immunohistochemical analysis for MMP-3 in cartilage. At 4 weeks, the positive cell rate in the ACL-T group was significantly increased compared with the Sham and the CATT groups. At 8 weeks, the positive cell rate in the ACL-T group was significantly increased compared with the Sham and the CATT groups, and that in the CATT group was significantly increased compared with the Sham group. Data are presented as the mean with a 95% CI. Black scale bar, 50 µm. (B) Immunohistochemical analysis for TNF-a in cartilage. At 2,4 and 8 weeks, there were no differences in the positive cell rate between all groups. Data are presented as the mean with a 95% CI. Black scale bar, 50 µm.

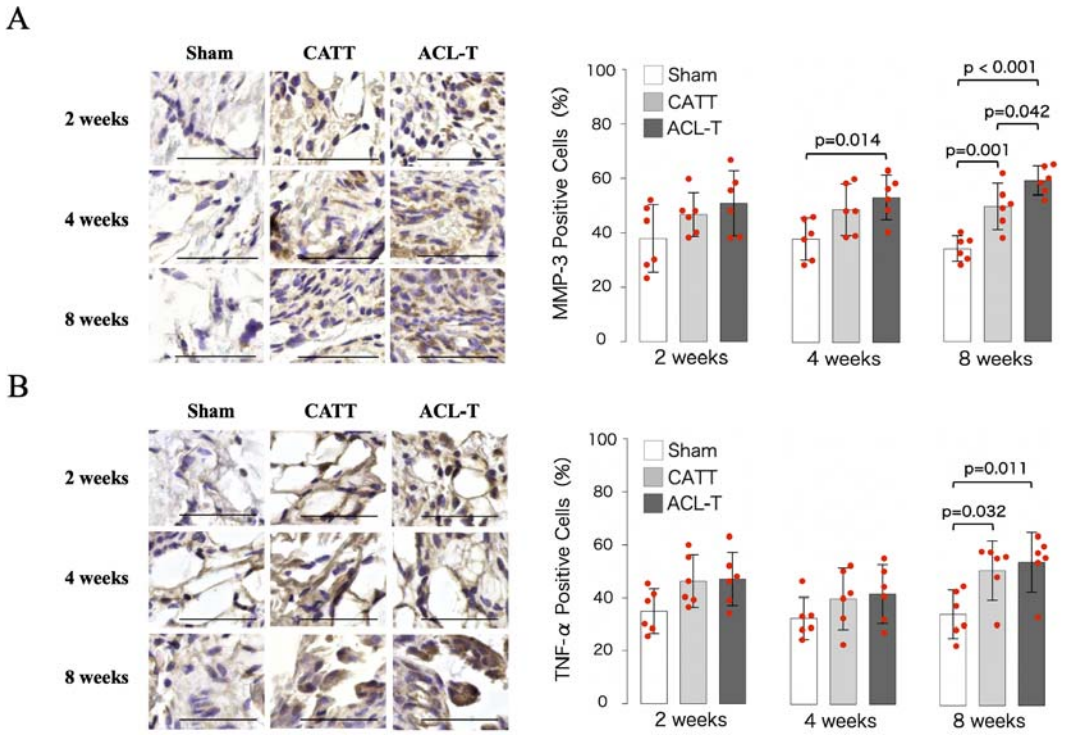

Figure 8. (A) Immunohistochemical analysis for MMP-3 in the synovium. At 4 weeks, the positive cell rate in the ACL-T group was significantly increased compared with the Sham group. At 8 weeks, the positive cell rate in the ACL-T group was significantly increased compared with the Sham and the CATT groups, and that in the CATT group was significantly increased compared with the Sham group. Data are presented as the mean with a 95% CI. Black scale bar, 50 µm. (B) Immunohistochemical analysis for TNF-a in the synovium. At 8 weeks, the positive cell rate in the CATT and the ACL-T group increased significantly compared to the Sham group. Data are presented as the mean with a 95% CI. Black scale bar, 50 µm.

Discussion

This study aimed to establish a novel Non-Invasive ACL-T model in mice without any injuries to intra-articular tissues and to elucidate the effect of shear stress on the onset mechanism of knee OA in the mice model. Our novel Non-Invasive ACL-T model showed no intra-articular damages such as cartilage degeneration, meniscus lesion, and bone loss at the subchondral bone. Next, we evaluated knee OA progression using this novel ACL-T model and the CATT model, which suppressed shear stress in the ACL-T model. As a result, the CATT group reduced cartilage degeneration and MMP-3 expression in articular cartilage and synovium compared to the ACL-T group.

However, there was no difference in synovitis and TNF-a in articular cartilage and synovium between the CATT and the ACL-T groups.

In a novel Non-Invasive ACL-T group, ACL rupture was observed histologically, and the amount of anterior tibial displacement was significantly increased compared with the INTACT group. A previous study using 14-16 weeks old C57BL/6 mice has revealed that the mean force applied for ACL rupture was 6.78±1.53 N and the failure speed was 10.90±4.37 N/s, as determined from the load cell data[23)]. Our data support this previous study for the rupture force, which may derive from applying a similar method to push the femoral condyle in the long axis. On the other hand, Christiansen et al. and Gilbert et al. have reported that it took 12N for ACL rupture in C57BL/6 mice from 10 to 12 weeks old using compression device[16,18)]. Our force was lower than the previous study using a compression device may attribute to differences in knee flexion degree and contact of joint surfaces[22)]. This study showed no difference between INTACT knees and ACL-T knees histologically, macroscopically, and morphologically. It has been reported that cartilage injuries occur in half, meniscus injuries in more than half, and subchondral fractures in 80% to 90% of ACL injuries. These injuries are attributed to compression stress by contact between femoral and tibial surfaces and result in apoptosis of chondrocytes, weakening the load distribution due to meniscal dysfunction, and changes in bone remodeling, leading to knee OA[24)]. These injuries may occur with previous Non-Invasive ACL-T models because ACL rupture was induced by applying compressive stress to the knee joint[16-18)]. Therefore, we needed to establish a novel, Non-Invasive ACL-T model without compression force during making the model assess the effects of pure shear stress on OA progression. This study set the knee joint at 90° of flexion, which can easily cause ACL rupture without the contact between the femoral and tibial surfaces. This method could create the model only pushing femoral condyle in the long axis direction. Thus, we successfully established a novel Non-Invasive ACL-T model inducing OA by shear stress in vivo.

Next, we examined the effects of shear stress on the onset of knee OA using this Non-Invasive model and the CATT model, which suppressed anterior tibial translation. Histological results showed that the OARSI score in the ACL-T group increased significantly compared with the CATT group at 8 weeks. The factors that cause knee OA after ACL injury include acute effects with cartilage lesion or subchondral bone damage and chronic mechanical impact caused by kinematic changes[25)]. The Non-invasive ACL-T model used in this study is guaranteed to be a model that causes no

intra-articular damage, including subchondral bone. On the other hand, the anterior drawer test showed that the amount of anterior tibial displacement in the ACL-T group increased significantly compared with the Sham and CATT groups at all weeks. Therefore, the cartilage degeneration in the ACL-T group at 8 weeks was most likely caused by the accumulation of abnormal mechanical stress, especially A-P direction shear stress. MMP-3 is a protease that triggers other MMP families by expressing early in knee OA and correlates with the severity of knee OA[4,26)]. In addition, it has also been reported that chondrocyte and synovial cells respond to shear stress and promote MMP-3[27,28)]. In this study, the positive cell rate of MMP-3 in chondrocytes increased at 4 weeks in the ACL-T group compared to the CATT group but not in synovial cells. The MMP-3 positive cell rates in chondrocytes and synovial cells were significantly increased at 8 weeks in the ACL-T group compared to the CATT group. These results suggest that chondrocytes are the first to respond to shear stress in vivo and cause cartilage degeneration.

Synovitis predates cartilage degeneration and is thought to be the source of intra-articular degeneration by propagating catabolic factors to chondrocytes via synovial fluid[10,11)]. Murata et al. have reported that the ACL-T group showed tissue thickening, more cell layers, and infiltration of inflammatory cells compared controlled joint group[29)]. Besides, Lifan et al. have reported that synovitis occurred as early as 1 week after destabilization of the medial meniscus (DMM), which preceded the events of cartilage degradation, subchondral sclerosis, and osteophyte formation[12)]. However, the relationship between cartilage degeneration and synovitis depends on the mechanical stress has not been revealed because the synovial invasive animal models were used in these studies. Interestingly, synovitis scores in the CATT and ACL-T groups were significantly higher than in the Sham group at 2 and 8 weeks. However, there was no difference between the CATT and ACL-T groups. In addition, although the positive cell rate of TNF-a in synovium in the CATT and ACL-T groups increased at 2 weeks and significantly increased at 8 weeks than the Sham group, there was no difference between the CATT and ACL-T groups. It has been reported that TNF-a alters synovial cells to an inflammatory phenotype and is released into synovial fluid soon after ACL injury[30)]. Therefore, synovitis in the CATT and ACL-T groups at 2 weeks may indicate that the acute inflammation associated with ACL rupture affected the synovial membrane through the synovial fluid. Chronic synovitis in knee OA generally results from the innate immune mechanism mediated by pattern recognition receptors located in synovium[31)]. Considering that there was no difference in the synovitis score between the CATT and ACL-T groups, it is suggested that the synovium does not respond

directly to mechanical stress in developing OA but rather causes inflammation in response to cartilage fragments released into the synovial fluid. In summary, it was suggested that synovitis in OA development by shear stress is not a primary mechanoresponse of local synovial cells but may be caused by the secondary response by cartilage fragments due to degeneration associated with the secondary response by cartilage fragments OA progression.

The limitation of this study is the inability to quantify the increase or decrease in mechanical stress. To evaluate the mechanism of knee OA, articular cartilage and synovium were selected for analysis. Still, the quantitation and mechanical stresses applied to each tissue may not be identical. Although our model reproduces the abnormal mechanical stress that occurs in vivo and thus is similar to the OA process in humans, in vitro experiments with quantified mechanical stress will be needed in the future.

Conclusion

We have successfully established a new Non-Invasive ACL-T model without intra-articular tissue damage, which induces knee OA due to shear stress. In OA progression induced by shear stress, chondrocytes first showed a molecular biological response in response to shear stress, leading to a local increase in MMP-3. Subsequently, we showed that MMP-3 might be increased in synovial cells through molecular biological interactions. Our results also suggest that mechanical stress does not directly induce synovitis but is indirectly caused by intra-articular degeneration associated with knee OA progression.

Citation

1. Blazek AD, Nam J, Gupta R, Pradhan M, Perera P, Weisleder NL, et al. Exercise-driven metabolic pathways in healthy cartilage. Osteoarthritis Cartilage. 2016;24(7):1210-22.
2. Tetsunaga T, Nishida K, Furumatsu T, Naruse K, Hirohata S, Yoshida. A, et al. Regulation of mechanical stress-induced MMP-13 and ADAMTS-5 expression by RUNX-2 transcriptional factor in SW1353 chondrocyte-like cells. Osteoarthritis and Cartilage. 2011;19(2):222-232.
3. Takeda Y, Niki Y, Fukuhara Y, Fukuda Y, Udagawa K, Shimoda M, et al. Compressive mechanical stress enhances susceptibility to interleukin-1 by increasing interleukin-1 receptor expression in 3D- cultured ATDC5 cells. BMC Musculoskelet Disord. 2021;22(1):238.
4. Ni GX, Zhan LQ, Gao MQ, Lei L, Zhou YZ, Pan YX. Matrix metalloproteinase-3 inhibitor

retards treadmill running-induced cartilage degradation in rats. Arthritis Res Ther. 2011;13(6): R192.

5. Chou CH, Jain V, Gibson J, Attarian DE, Haraden CA, Yohn CB, et al. Synovial cell cross-talk with cartilage plays a major role in the pathogenesis of osteoarthritis. Sci Rep. 2020;10(1):10868.
6. Hugle T, Geurts J. What drives osteoarthritis?-synovial versus subchondral bone pathology. Rheumatology. 2017;56(9):1461-71.
7. Lu J, Zhang H, Cai D, Zeng C, Lai P, Shao Y, et al. Positive- Feedback Regulation of Subchondral H-Type Vessel Formation by Chondrocyte Promotes Osteoarthritis Development in Mice. J Bone Miner Res. 2018;33(5):909-20.
8. Zhang H, Wang H, Zeng C, Yan B, Ouyang J, Liu X, et al. mTORC1 activation downregulates FGFR3 and PTH/PTHrP receptor in articular chondrocytes to initiate osteoarthritis. Osteoarthritis Cartilage. 2017;25(6):952-63.
9. Cui Z, Crane J, Xie H, Jin X, Zhen G, Li C, et al. Halofuginone attenuates osteoarthritis by inhibition of TGF-beta activity and H- type vessel formation in subchondral bone. Ann Rheum Dis. 2016;75(9):1714-21.
10. Carla R, Steven R. The role of synovitis in osteoarthritis pathogenesis. Bone. 2012 Aug;51(2):249-57.
11. Alexander M, Philip G. Synovitis in osteoarthritis: current understanding with therapeutic implications. Arthritis Research & Therapy volume. 2017;19:18
12. Lifan L, Shanxing Z, Lan Z, Xiaofeng C, Lin H, Jian H, et al. Acute Synovitis after Trauma Precedes and is Associated with Osteoarthritis Onset and Progression. Int J Biol Sci. 2020; 16(6): 970–980.
13. Kokubun T, Kanemura N, Murata K, Moriyama H, Morita S, Jinnno T, et al. Effect of Changing the Joint Kinematics of Knees With a Ruptured Anterior Cruciate Ligament on the Molecular Biological Responses and Spontaneous Healing in a Rat Model. Am J Sports Med. 2016 Nov;44(11):2900-2910.
14. Arakawa K, Takahata K, Enomoto S, Oka Y, Ozone K, Morosawa K, et al. Effect of Suppression of Rotational Joint Instability on Cartilage and Meniscus Degeneration in Mouse Osteoarthritis Model. Cartilage. Jan-Mar 2022;13(1)
15. Arakawa K, Takahata K, Enomoto S, Oka Y, Ozone K, Nakagaki S, et al. The difference in joint instability affects the onset of cartilage degeneration or subchondral bone changes. Osteoarthritis Cartilage. 2022 Mar;30(3):451-460.
16. Christiansen B, Anderson J, Lee A, Williams C, Yik J, Haudenschild D. Musculoskeletal changes following non-invasive knee injury using a novel mouse model of post-traumatic osteoarthritis. Osteoarthritis Cartilage. 2012 Jul;20(7):773-82.

17. Maerz T, Newton M, Kurdziel M, Altman P, Anderson A, Matthew H, et al. Articular cartilage degeneration following anterior cruciate ligament injury: a comparison of surgical transection and non-invasive rupture as preclinical models of post-traumatic osteoarthritis. Osteoarthritis Cartilage. 2016 Nov;24(11):1918-1927.
18. Sophie J, Cleo S, Paulina S, Victor C, Deborah J, Emma J, et al. Inflammatory and degenerative phases resulting from anterior cruciate rupture in a non-invasive murine model of post-traumatic osteoarthritis. J Orthop Res. 2018 Feb 17;36(8):2118-2127.
19. Udo M, Muneta T, Tsuji K, Ozeki N, Nakagawa Y, Ohara T, et al. Monoiodoacetic acid induces arthritis and synovitis in rats in a dose- and time-dependent manner: proposed model-specific scoring systems. Osteoarthritis Cartilage. 2016;24(7):1284-91.
20. Glasson S, Chambers M, Van W, Little C. The OARSI histopathology initiative - recommendations for histological assessments of osteoarthritis in the mouse. Osteoarthritis Cartilage. 2010;18 Suppl 3:S17-23.
21. Krenn V, Morawietz L, Burmester G, Kinne R, Mueller U, Muller B, et al. Synovitis score: discrimination between chronic low-grade and high-grade synovitis. Histopathology. 2006;49(4):358-64.
22. Allison W, Franklin D, Trevor J, Priscilla M, Blaine A. Comparison of Knee Injury Threshold During Tibial Compression Based on Limb Orientation in Mice. J Biomech. 2018; 74: 220–224.
23. Xueying Z, Xiang D, Zhe S, Brett C, Camila C, Zoe A, et al. Matrix Metalloproteinase Inhibition With Doxycycline Affects the Progression of Posttraumatic Osteoarthritis After Anterior Cruciate Ligament Rupture: Evaluation in a New Nonsurgical Murine ACL Rupture Model. Am J Sports Med. 2020 Jan;48(1):143-152.
24. Wang LJ, Zeng N, Yan ZP, Li JT, Ni GX. Post-traumatic osteoarthritis following ACL injury. Arthritis Res Ther. 2020;22(1):57.
25. Luc B, Gribble PA, Pietrosimone BG. Osteoarthritis prevalence following anterior cruciate ligament reconstruction: a systematic review and numbers-needed-to-treat analysis. J Athl Train. 2014;49(6):806-19.
26. Cabral-Pacheco GA, Garza-Veloz I, Castruita-De la Rosa C, Ramirez-Acuna JM, Perez-Romero BA, Guerrero-Rodriguez JF, et al. The Roles of Matrix Metalloproteinases and Their Inhibitors in Human Diseases. Int J Mol Sci. 2020;21(24).
27. Iseki T, Rothrauff B, Kihara S, Sasaki H, Yoshida S, Fu F, et al. Dynamic Compressive Loading Improves Cartilage Repair in an In Vitro Model of Microfracture: Comparison of 2 Mechanical Loading Regimens on Simulated Microfracture Based on Fibrin Gel Scaffolds Encapsulating Connective Tissue Progenitor Cells. Am J Sports Med. 2019 Jul;47(9):2188-2199.
28. Sun H, Yokota H. Messenger-RNA expression of matrix metalloproteinases, tissue inhibitors of metalloproteinases, and transcription factors in rheumatic synovial cells under mechanical

stimuli. Bone. 2001 Mar;28(3):303-9.

29. Murata K, Kokubun T, Onitsuka K, Oka Y, Kano Y, Morishita Y, et al. Controlling joint instability after anterior cruciate ligament transection inhibits transforming growth factor-beta-mediated osteophyte formation. Osteoarthritis Cartilage. 2019 Aug;27(8):1185-1196.
30. Cameron M, Buchegraber A, Passler H, Vogt M, Thonar E, et al. The Natural History of the Anterior Cruciate Ligament-Deficient Knee- Changes in Synovial Fluid Cytokine and Keratan Sulfate Concentrations. Am J Sports Med. 1997;25(6):751-4.
31. Scanzello C, Plass A, Crow M. Innate immune system activation in osteoarthritis- is osteoarthritis a chronic wound?. Curr Opin Rheuumatol. 2008;20(5):565-72.